Functional Materials 20, No.4 (2013) 

# Light scattering by residual pores in $Y_2O_3$ nanograined ceramics

***R.P.Yavetskiy, O.L.Shpilinskaya, V.N.Baumer, A.G.Doroshenko, A.V.Tolmachev, I.A.Petrusha*, V.Z.Turkevich****

STC "Institute for Single Crystals", Institute for Single Crystals, National Academy of Sciences of Ukraine, 60 Lenin Ave., 61001 Kharkiv, Ukraine
*V.Bakul Institute for Superhard Materials, National Academy of Sciences of Ukraine, 2 Avtozavodskaya Str., 04074 Kyiv, Ukraine

*Received October 18, 2013*

Correlation between the in-line optical transmittance and residual porosity of $Y_2O_3$ nanoceramics formed by high-pressure low-temperature sintering has been established. In the limit case, when the pore diameter is much smaller than the wavelength a formula for estimating the porosity at the known value of linear transmittance was obtained. For investigated samples of nanograin composite ceramics with average grain size of 10–20 nm, the pore size of 12 nm and linear transmittance of 50 % at wavelength of 900 nm the calculated value of residual porosity was 0.27 %. Phase composition of $Y_2O_3$ nanoceramics may be taken into account by varying refractive index of the composite ceramics containing both cubic and monoclinic yttria.

Установлена корреляция между линейным оптическим пропусканием и остаточной пористостью нанокерамик $Y_2O_3$, формируемых методом спекания при высоких давлениях. В предельном случае, когда диаметр пор много меньше длин волн, в рамках теории Ми получена формула для оценки пористости при известном значении линейного пропускання. Для исследуемых образцов композитной нанозеренной керамики со средним размером зерна 10–20 нм, размером пор 12 нм и линейным коэффициентом оптического пропускания 50 % на длине волны 900 нм расчетное значение остаточной пористости составило 0,27 %. Фазовый состав керамики может быть учтен путем вариации показателя преломления композитной нанокерамики, содержащей как кубическую, так и моноклинную модификацию $Y_2O_3$.

***Розсіяння світла залишковими порами у нанозеренній кераміці $Y_2O_3$.*** *Р.П.Явецький, О.Л.Шпилинська, В.М.Баумер, А.Г.Дорошенко, О.В.Толмачев, І.А.Петруша, В.З.Туркевич.*

Встановлено кореляцію між лінійним оптичним пропусканням та залишковою пористістю нанокераміки $Y_2O_3$, яка сформована методом спікання при високих тисках. У граничному випадку, коли діаметр пор значно менше довжин хвиль, в рамках теорії Мі одержано формулу для оцінки пористості при відомому значенні лінійного пропускання. Для досліджених зразків композитної нанозеренної кераміки з середнім розміром зерна 10–20 нм, розміром пор 12 нм та лінійним коефіцієнтом оптичного пропускання 50 % на довжині хвилі 900 нм розраховане значення залишкової пористості складає 0,27 %. Фазовий склад кераміки може бути враховано шляхом варіації показника заломлення композитної нанокераміки, що містить як кубічну, так і моноклінну модифікацію $Y_2O_3$.

## 1. Introduction

Recently optical ceramics containing negligible concentration of residual pores have been actively studied as a new class of functional materials for photonics, laser, scintillation techniques, etc. [1]. Properties of ceramics as an optical medium are determined mainly by their microstructure, namely the presence of impurity phases, grain size, grain boundary width, pore size and concentration. Utilization of advanced ceramic technologies allows one to form the phase-pure ceramics with narrow grain boundaries (1 nm), in which residual pores serve as the main scattering centers. Nanograined ceramics attract considerable attention not only due to better mechanical properties compared with coarse-grained analogues, but also owing to potentially improved transparency because of lower light scattering on pores with a size much smaller than the visible light wavelength [2]. According to [3, 4] even relatively low dense $MgAl_2O_4$ nanograined ceramics with $\rho = 98–99$ % may achieve high transparency ($T \approx 80$ %). At the same time to obtain the transparency comparable to single crystals micron-sized ceramics have to be at least 99.985 % dense [5, 6]. Obviously, the decrease in pore size from submicron to nanometer range at fixed porosity value is responsible for higher transparency of nanoceramics, but even the nanoscale pores have a significant effect on their optical transmission [7]. Therefore, establishing quantitative relationships between porosity and transmittance is an important problem that will allow optimizing the manufacturing technology of the optical nanoceramics.

Evaluation of porosity of the nanoceramics by experimental methods is a difficult and time consuming task. Some studies estimate the porosity by analyzing micrographs of pores plane sections [8]. Determination of the porosity by pores plane sections can be done using stereological methods [9]. However, it seems, these methods are unacceptable to investigate nanograined ceramics due to the nonuniform distribution of the pores throughout the sample volume and higher concentration in the bulk in comparison with the surface [10]. Consequently, different cross sections may have different pore distribution law, while the analysis of the mechanisms of pore formation can not provide adequate hypothesis about the distribution of the pore centers. However, hypothesis that the pores have a shape close to spherical, and their centers are located at distances much longer than wavelengths are in good agreement with the experimental data. In the case of monodispersed pores with the spherical shape, and assuming that pore diameter and the distance between their centers is much smaller than wavelengths the porosity can be evaluated by certain transparency. Recently transmission of $Al_2O_3$, $ZrO_2$ nanograined ceramics depending on the pore sizes has been studied in the framework of the Mie, Rayleigh and Rayleigh-Gans-Debye light scattering models [7, 11–13]. This work is devoted to assessment of porosity of $Y_2O_3$ nanoceramics, a promising material for solid-state lasers and transparent phosphors [14], by analyzing their in-line transmission.

## 2. Experimental

$Y_2O_3$ nanograined ceramics were fabricated by transformation-assisted consolidation of 125 nm discrete nanospheres under high-pressure according to [15]. Briefly, cubic yttria nanopowder with specific surface of 17 $m^2/g$ and average crystallite size of $d_{XRD} \approx 40$ nm were used as a starting material. After being compacted under the pressure of 250 MPa the green bodies were placed in the toroid-type high pressure cell and sintered under 8 GPa pressure at temperatures within 25–500°C range for 30–300 s in a high-pressure apparatus. Phase identification was performed via X-ray diffraction (XRD) method on SIEMENS D-500 X-ray diffractometer ($CuK\alpha$ radiation, graphite monochromator) on the powdered ceramic samples. The phases were identified using JCPDS PDF-1 card file and EVA retrieval system included in the diffractometer software. The Rietveld refinement was performed with FullProf program. The ceramics microstructure was studied by high-resolution analytical transmission electron microscopy (HR TEM) on JEM-2100F (JEOL) microscope. The samples for the HR TEM were prepared by ion thinning. Optical measurements were performed on 1 mm thick ceramic plates with polished surfaces. In-line optical transmission of the samples was determined using Perkin-Elmer "LAMBDA-35" spectrophotometer in 200–1000 nm wavelength range. Porosity of the samples obtained was evaluated in the extreme case of Mie scattering theory.

## 3. Results and discussion

### 3.1. Theoretical research

Theoretical dependency of transmission on wavelength can be described by the Beer-Lambert law

$$T = (1 - R)^2 \exp(-C_{sca} \cdot t), \quad (1)$$

where $R = (m-1)^2/(m+1)^2$ — reflectivity, $m = n_{air}/n_{med}$, $n_{med}$ — refractive index of the media, $n_{air}$ — refractive index of the air, $C_{sca}$ — effective scattering coefficient, $t$ — sample thickness.

Effective scattering coefficient depends on many factors especially on geometry and ceramics pore size. Next we will consider that the diameter of all pores is constant and small comparing with the wavelength. We also suppose that the distance between pore centers is much more than the wavelength and pores have got sphere shape. Within the frameworks of the made hypotheses the scattering efficiency is connected with pore diameter $d$, porosity $V_{pore}$ and scattering efficiency $Q_{sca}$ for one pore in the following way [13]:

$$C_{sca} = \frac{3 \cdot V_{pore}}{2 \cdot d} \cdot Q_{sca}. \quad (2)$$

Using formula (1) for scattering coefficient in the equation we can get dependency of transmission on the efficiency coefficient and porosity:

$$T = (1 - R)^2 \exp\left(-\frac{3 \cdot V_{pore}}{2 \cdot d} Q_{sca} \cdot t\right). \quad (3)$$

For calculating scattering efficiency the Mie scattering theory can be used. According to this theory the scattering efficiency can be represented by integration of the amplitude functions $S(\theta,\varphi)$[16]

$$C_{sca} = \int_0^{2\pi} \int_0^{\pi} \frac{|S(\theta,\varphi)|^2}{k^2} \sin\theta d\theta d\varphi. \quad (4)$$

Fig. 1 illustrates the dependence of scattering efficiency on wavelength for the sphere-shaped pores of different diameters. The scattering efficiency calculations were conducted using the Mie theory according to the standard algorithms described in [16]. As can be seen, the residual porosity has great influence on the transmission. Fig. 2 describes the dependence of transmission at 400, 600 and 800 nm wavelength on pore size assuming different porosity level. One can conclude that decrease of the porosity level results in improved transmission.

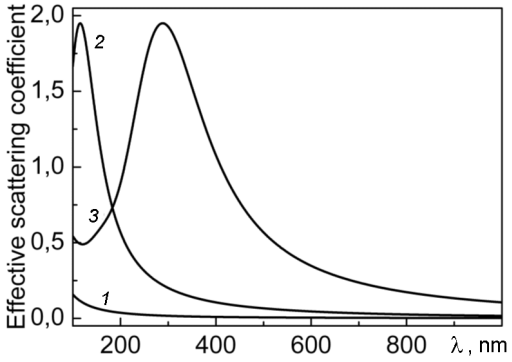


Fig. 1. Dependence of scattering efficiency on wavelength for spherical-shaped pore with diameters of 12 nm (*1*), 40 nm (*2*) and 100 nm (*3*).

In general case of the Mie theory the scattering efficiency is expressed by the Bessel functions. If the pore diameters are small as compared to wavelength, approximation up to terms of $x^4$ order is acceptable

$$Q_{sca} = \frac{8}{3} \cdot x^4 \cdot \left|\frac{m^2 - 1}{m^2 + 1}\right|^2, \quad x = \frac{d \cdot \pi \cdot n_{med}}{\lambda}, \quad (5)$$

where λ is wavelength. In this case by adding to the formula (3) an explicit expression for $Q_{sca}$ from the relation (5) we can get the dependency of transmission on characteristic parameters of the nanoceramics.

$$T = (1 - R)^2 \exp\left(-\frac{4 \cdot d^3(\pi \cdot n_{med})^4 \cdot t}{\lambda^4} \cdot \left|\frac{m^2 - 1}{m^2 + 1}\right|^2 \cdot V_{pore}\right). \quad (6)$$

Let $C = 4 \cdot d^3(\pi \cdot n_{med})^4 \cdot t \cdot \left|\frac{m^2 - 1}{m^2 + 1}\right|^2$.

We should note that if $\lambda >> C \cdot V_{pore}$, the exponent in (6) is quite different from 0, in this limit case the transmission is $T \approx (1 - R)^2$. Let consider another limit case when $\lambda << C \cdot V_{pore}$. On such wavelengths the exponent $C \cdot V_{pore}/\lambda^4$ is increasing without limit, so the transmission $T$ on such wavelength is tending to 0. In the $\lambda \approx C \cdot V_{pore}$ wavelength range the transmission is greatly influenced by the porosity that can be expressed as follows (assuming that $x$ have small values):

$$V_{pore} = \frac{d \cdot (m^2 + 2)^2}{2 \cdot x^4 \cdot t \cdot (m^2 - 1)^2} \cdot \ln\left|\frac{1 - R}{T}\right|, \quad (7)$$

$$x = \frac{d \cdot \pi \cdot n_{med}}{\lambda^4}.$$

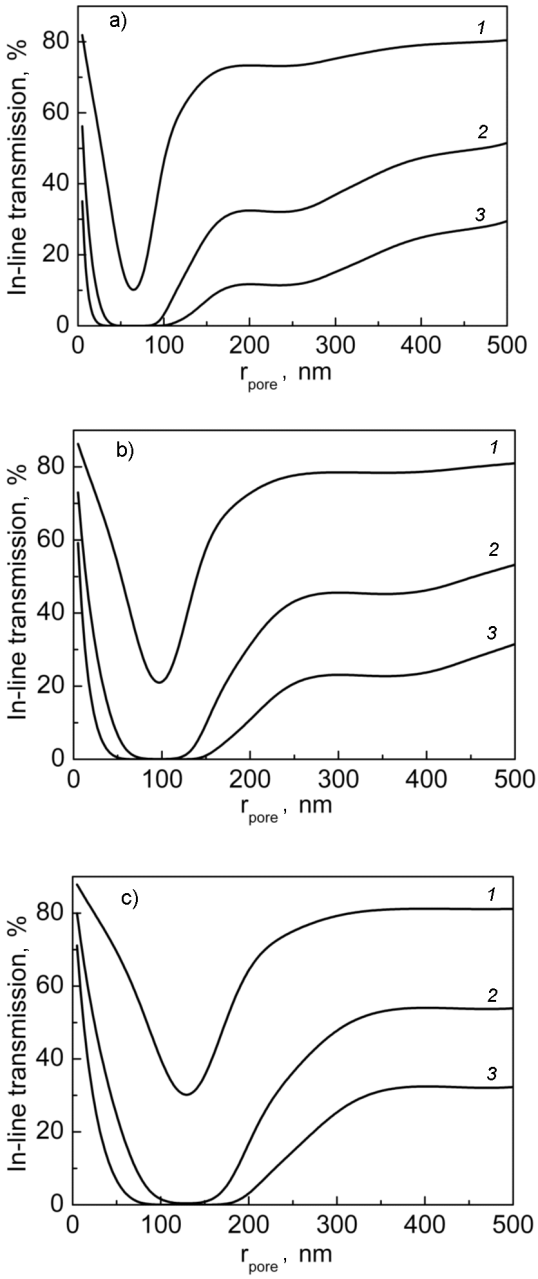


Fig. 2. Transmission at 400 (a), 600 (b) and 800 nm (c) wavelength depending on pore radius assuming the porosity of 0.01 % (*1*), 0.05 % (*2*) and 0.1 % (*3*).

Thus, when the pore dimensions are significantly less than the wave length the porosity can be evaluated according to (7).

### *3.2. Obtaining and characterization of $Y_2O_3$ nanoceramics*

Transformation-assisted consolidation of yttria nanopowders under high pressure which is considered as one of the most promising approaches to retain nanostructure of materials was used to manufacture $Y_2O_3$ optical nanograined ceramics. According to XRD data $Y_2O_3$ ceramics sintered under $P = 8$ GPa, $T = 300$°C and $t = 30$ s is biphasic and contains yttria in cubic (C) and monoclinic modification (B) with C/B ≈ 1:3. Obtained composite ceramics was characterized by the following lattice parameters: C–$Y_2O_3$: $a = 10.6091(7)$ Å, $V = 1194.08(15)$ Å$^3$; $d = 18$ nm; B–$Y_2O_3$:$a = 13.8625(14)$, $b = 3.5107(3)$, $c = 8.6097(9)$ Å, $\beta = 100.151(7)°$, $V = 412.45(7)$ Å$^3$, $d = 9$ nm. The determined lattice parameters were found to be in a good agreement with the calculated data [17, 18]. High nucleation rate of monoclinic phase inside the volume of parent cubic yttrium oxide stabilizes the unprecedented low crystallite size even smaller than that of the initial nanopowders, while rearrangement of the crystal lattice during C → B phase transformation reduces the resistance of plasticity and provides effective densification. As a result, the sintered ceramics achieves near theoretical density of 99±1 % within the measurement method error. Fig. 3 shows photograph of the ceramics obtained under optimized conditions

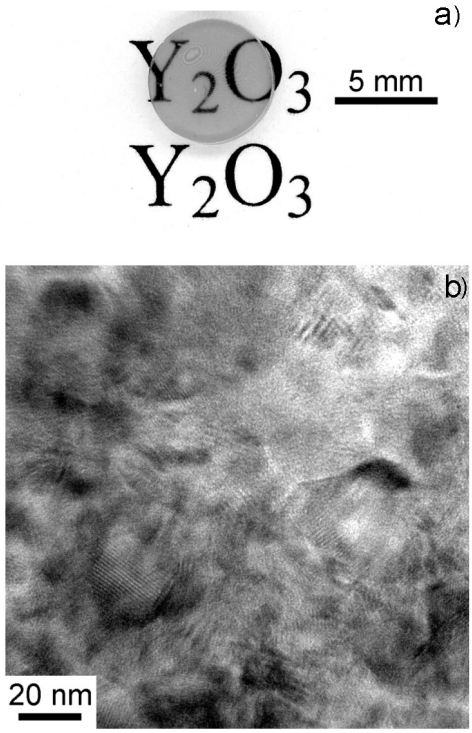


Fig. 3. 1 mm-thick $Y_2O_3$ nanograined ceramics obtained at $P = 8$ GPa, $T = 300$°C, $t = 30$ s (a) and HR TEM image of $Y_2O_3$ nanoceramics (b), arrow indicate a pore.

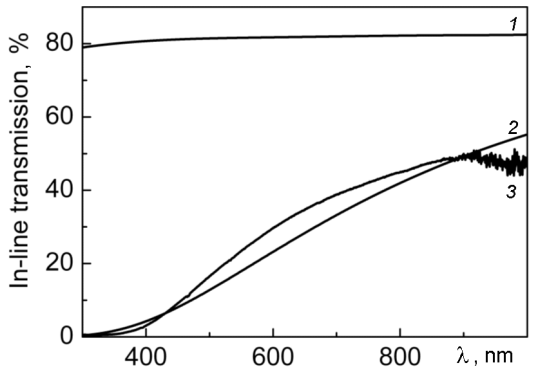


Fig. 4. Experimental (*3*), calculated (*2*) and theoretical (*1*) in-line optical transmission of $Y_2O_3$ nanograined ceramics.

as well as its morphology at nanoscale. The ceramics is transparent and the text is clearly seen through it. The grain size, as determined from the micrograph in Fig. 3b lies within 10–20 nm range, which agrees well with average crystallite size determined by XRD method (about 10 nm for the monoclinic and 20 nm for the cubic modification). According to HR TEM the samples of nanoceramics virtually does not contain micron and submicron pores, but has uniformly distributed pores with a characteristic size of about 12 nm (Fig. 3b, arrow). The average pore size of $Y_2O_3$ nanoceramics formed by the consolidation of nanopowders under high pressures is of the same order of magnitude as that for other consolidated nanomaterials obtained by high pressure sintering [19, 20].

Fig. 4 demonstrates the estimated and experimental real in-line transmission spectra of synthesized $Y_2O_3$ nanoceramics for the fixed sample thickness of 1 mm. The experimental curve of optical transmission is practically monotonically increasing and reaches 50 % at 900 nm wavelength (Fig. 4 curve *3*). This value achieves 60 % from the theoretical value of transmission of non-porous $Y_2O_3$ (82.3 %, Fig. 4 curve *1*), that was calculated using data on dispersion of refraction index [21]. Red shift of the fundamental absorption edge of yttria nanoceramics +from 250 nm [22] to about 300 nm may be related to the presence of color centers generated by reducing conditions during high-pressure sintering [23] or to light scattering by residual nanometeric pores [7].

To estimate the porosity according to the transmission curve 395–570 nm wavelength range with the strongest transmission growth was selected. According to Fig. 1

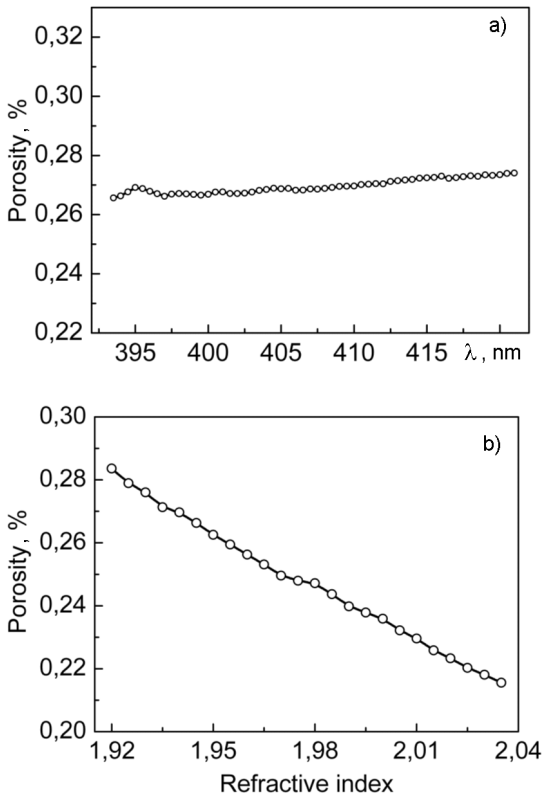


Fig. 5. Porosity of $Y_2O_3$ nanoceramics estimated in accordance with the in-line optical transmission (a) and influence of the refraction coefficient on porosity of $Y_2O_3$ composite ceramics (b).

the transmission efficiency curve $Q_{sca}(\lambda)$ for $d = 12$ nm is decreasing with the wavelength increase. So such pores have a greatest impact on scattering at the smaller wavelength. This means that for the sample analyzed we should estimate the porosity at the beginning of the selected interval. For $Y_2O_3$ nanoceamics studied $2\pi n_{med} r/\lambda$ ratio is changing within the limits of 0.39÷0.42 in the 395–420 nm wavelength range. Therefore this ratio can be considered as a small one that allows us to use equation (7) for the porosity assessment. Fig. 5a presents a curve calculated using formula (7). According to the obtained dependency we can conclude that the sample porosity is about 0.27 %. The transmission curve in Fig. 5b was calculated for estimated porosity value taking into account the foregoing suggestions about the pore sizes and distances between their centers. The little difference between experimental and theoretical curves may come due to the fact that generally the pore diameter is random variable.

Since the ceramics consist of cubic and monoclinic phases having different refractive indices the additional light losses occur due to birefringence. The refraction coefficient of the monoclinic modification is unknown due to the difficulties of growing high-quality single crystals [24]. However, yttrium oxide thin films containing both cubic and monoclinic modifications have higher refractive index compared with the cubic yttrium oxide films. Consequently, the refractive index of the composite ceramics increases compared with single-phase cubic $Y_2O_3$ [25]. Fig. 5b shows the dependence of the porosity on the refractive index calculated according to (7). Refractive index increase results in lower residual porosity of the nanoceramics. Thus, using $n$ for cubic $Y_2O_3$ nanoceramics gives an upper estimate of the residual porosity. The residual porosity value lies within 0.256–0.260 % range when $n_{med} = 1.95–1.96$ typical for (C + B)$Y_2O_3$ system [25] is applied.

## *4. Conclusion*

Composite $Y_2O_3$ nanograined ceramics containing cubic and monoclinic phases has been obtained by transformation-assisted sintering of nanopowders under 8 GPa. The nanoceramics is characterized by in-line optical transmission of 50 % at 900 nm achieving 60 % from the theoretical value, and the average pore size of about 12 nm. In the framework of the Mie scattering theory using the Beer-Lambert low a formula to estimate the residual porosity using measured optical transmission has been deduced. According to (7) calculation value of porosity for the synthesized yttria nanoceramics was found to be 0.27 %. Phase composition of the ceramics can be taking into account by variation of the refractive index.

*Acknowledgments*. The authors would like to thank to Dr.M.I.Danylenko for the help in testing experimental samples by HR TEM.

## *References*

1. A.Ikesue, Y.L.Aung, *Nature Photonics*, **2**, 721 (2008).
2. G.L.Messing, A.J.Stevenson, *Science*, **322**, 383 (2008).
3. T.C.Lu, X.H.Chang, J.Q.Qi et al., *Appl. Phys. Lett.*, **88**, 213120 (2006).
4. J.Zhang, T.C.Lu, X.H.Chang et al., *J. Phys. D: Appl. Phys.*, **42**, 052002 (2009).
5. A.Ikesue, K.Yoshida, *J. Mater. Sci.*, **34**, 1189 (1999).
6. R.Boulesteix, A.Maotre, J.-F.Baumard et al., *Opt. Exp.*, **18**, 14992 (2010).
7. U.Anselmi-Tamburini, J.N.Woolman, Z.A.Munir, *Adv. Funct. Mater.*, **17**, 3267 (2007).
8. W.Zhang, T.Lu, N.Wei et al., *J. Alloys and Compd.*, **520**, 36 (2012).
9. D.G.Kendall, E.F.Hardin, Stohastic Geometry, J. Wiley&Sons, London (1974).
10. P.G.Cheremskoy, V.V.Slyozov, V.I.Betekhin, Pores in Solids, Energoatomizdat, Moscow (1990) [in Russian].
11. R.Apetz, M.P.B.van Bruggen, *J. Am. Ceram. Soc.*, **86**, 480 (2003).
12. J.Klimke, M.Trunec, A.Krell, *J. Am. Ceram. Soc.*, **94**, 1850 (2011).
13. I.Yamashitai, K.Tsukuma, *J. Ceram. Soc. Jpn.*, **119**, 133 (2011).
14. J.Luo, Z.Zhong, J.Xu, *Mat. Res. Bull.*, **47**, 4283 (2012).
15. R.P.Yavetskiy, V.N.Baumer, N.A.Dulina et al., *J. Eur. Ceram. Soc.*, **32**, 257 (2012).
16. C.F.Bohren, D.R.Huffman, Absorption and Scattering of Light by Small Particle, Wiley, New York (1983).
17. H.Yusa, T.Tsuchiya, N.Sata et al., *Inorg. Chem.*, **49**, 4478 (2010).
18. P.P.Bose, M.K.Gupta, R.Mittal et al., *Phys. Rev. B*, **84**, 094301 (2011).
19. A.V.Ragulya, *Adv. Appl. Ceram.*, **107**, 118 (2008).
20. R.P.Yavetskiy, E.A.Vovk, A.G.Doroshenko et al., *Ceram. Int.*, **37**, 2477 (2011).
21. Y.Nigara, *Jpn. J. Appl. Phys.*, **7**, 404 (1968).
22. T.Tomiki, J.Tamashiro, Y.Tanahara et al., *J. Phys. Soc. Jpn.*, **55**, 4543 (1986).
23. R.Peters, K.Petermann, G.Hubert, in: P.Capper, P.Rudolph (Eds.), Crystal Growth Technology: Semiconductors and Dielectrics, Wiley-VCH, Weinheim (2010).
24. V.Srikantha, A.Sato, J.Yoshimoto et al., *Cryst. Res. Technol.*, **29**, 981 (1994).
25. A.Og.Dikovska, P.A.Atanasov, I.G.Dimitrov et al., *Appl. Surf. Sci.*, **252**, 4569 (2006).